Article

Lipidated Peptide Dendrimers Killing Multidrug Resistant Bacteria

Thissa N. Siriwardena, Michaela Stach, Runze He, Bee-Ha Gan, Sacha Javor, Marc Heitz, Lan Ma, Xiangjun Cai, Peng Chen, Dengwen Wei, Hongtao Li, Jun Ma, Thilo Koehler, Christian van Delden, Tamis Darbre, and Jean-Louis Reymond

J. Am. Chem. Soc., **Just Accepted Manuscript** • DOI: 10.1021/jacs.7b11037 • Publication Date (Web): 05 Dec 2017

Lipidated Peptide Dendrimers Killing Multidrug Resistant Bacteria

Thissa N. Siriwardena,[a)] Michaela Stach,[a)] Runze He,[a) b)] Bee-Ha Gan,[a)] Sacha Javor,[a)] Marc Heitz,[a)] Lan Ma,[b) c) d)] Xiangjun Cai,[c)] Peng Chen,[e)] Dengwen Wei,[e)] Hongtao Li,[e)] Jun Ma,[c)] Thilo Köhler,[f)] Christian van Delden,[f)] Tamis Darbre[a)]* and Jean-Louis Reymond[a)]*

[a)] *Department of Chemistry and Biochemistry, University of Bern, Freiestrasse 3, 3012 Bern, Switzerland. e-mail: jean-louis.reymond@dcb.unibe.ch*

[b)] *Shanghai Space Peptides Pharmaceutical Co. Ltd, Shanghai, China*

[c)] *College of Pharmacy, GanSu University of Chinese Medicine, Dingxi east road 35, Chenguan district, Lanzhou, China*

[d)] *Lanzhou Ruibei Pharmaceutical R&D Co., Ltd., Lanzhou, China*

[e)] *Department of General Surgery, Lanzhou General Hospital of Lanzhou Military Region, PLA, 333 South Binhe Road, Qilihe District, Lanzhou, Gansu Province, China*

[f)] *Department of Microbiology and Molecular Medicine, University of Geneva, and Service of Infectious Diseases, University Hospital of Geneva, Geneva, Switzerland*

Abstract

New antibiotics are urgently needed to address multidrug resistant (MDR) bacteria. Herein we report that second generation (G2) peptide dendrimers bearing a fatty acid chain at the dendrimer core efficiently kill Gram-negative bacteria including *Pseudomonas aeruginosa* and *Acinetobacter baumannii,* two of the most problematic MDR bacteria worldwide. Our most active dendrimer **TNS18** is also active against Gram-positive methicillin resistant *Staphylococcus aureus* (MRSA). Based on circular dichroism and molecular dynamics studies we hypothesize that **TNS18** adopts a hydrophobically collapsed conformation in water with the fatty acid chain backfolded onto the peptide dendrimer branches, and that the dendrimer unfolds in contact with the membrane to expose its lipid chain and hydrophobic residues, thereby facilitating membrane disruption leading to rapid bacterial cell death. Dendrimer **TNS18** shows promising in vivo activity against MDR clinical isolates of *A. baumannii* and *E. coli,* suggesting that lipidated peptide dendrimers might become a new class of antibacterial agents.

Introduction

Multidrug resistant (MDR) *Pseudomonas aeruginosa* and *Acinetobacter baumannii* have been listed, together with *Enterobacteriaceae,* as the most critical human pathogens in a February 2017 call for new antibiotics by the World Health Organization. Most approaches currently available to address this call rely on screening natural product sources such as soil bacteria or small molecule drug libraries, which comprise molecules either made by nature or closely related to known drugs and natural products.[1-3]

One important alternative consists in designing analogs of antimicrobial peptides (AMPs), a broad class of naturally occurring cyclic or linear peptides which mostly kill bacteria by a membrane disruptive mechanism.[4-8] These designed analogs are expected to overcome the typical limitations of peptides in terms of stability. Most reports to date exploited classical linear or cyclic chain topologies while introducing alternative building blocks such as D-enantiomeric[9-12] and β-amino acids,[13] peptoids,[14-20] nylon,[21, 22] or urea linked diamines.[23, 24] In our approach by contrast, we explore unusual multibranched topologies of the peptide chain, such as peptide dendrimers and bicyclic peptides, while keeping building blocks constant.[25-27] Extending on previous reports that multivalent display of AMPs on a poly-lysine tree can increase their antimicrobial activity,[28-30] we recently identified the third generation (G3) antimicrobial peptide dendrimer (AMPD) **G3KL** consisting of a lysine-leucine dipeptide repeated across the dendrimer branches active against *P. aeruginosa* and *A. baumannii* laboratory strains,[31] as well as against a broad panel of multidrug resistant clinical isolates of both of these pathogens,[32] and with favorable pro-angiogenic properties in biological burn-wound bandages.[33]

We had initially obtained **G3KL** by exploiting a dendritic effect on antimicrobial activity, i.e. an increase in antibacterial activity with dendrimer generation, with the consequence that **G3KL** was relatively large and difficult to synthesize in high yields. Here we set out to search for a smaller but equally active version of this AMPD by focusing on the second generation (G2) peptide

dendrimer **G2KL**, which only showed activity against *P. aeruginosa* in LB (Luria-Bertani) medium, but not in MH (Müller-Hinton) medium which is more relevant to antibiotic use, probably due to the higher magnesium ion concentration. To increase the activity of **G2KL**, we investigated the effect of adding a short fatty acid chain to the dendrimer because such fatty acid chains are found in many AMPs where they play an essential role for their activity,[34, 35] including the case of polymyxin B, a last resort cyclic peptide antibiotic against Gram-negative MDR bacteria used here as a positive control, but against which resistance is appearing.[36-39] Furthermore lipidation is often used to extend the circulation time of peptides in vivo by inducing binding to serum albumin,[40] which extends their circulation time as demonstrated for insulin[41] as well as for GLP-1 analogues.[42]

Here we report how the addition of a fatty acid to the core of **G2KL** followed by a combinatorial sequence optimization led us to discover AMPD **TNS18**, which is only half the size of **G3KL** yet displays a broader antibacterial activity spectrum including not only Gram negative MDR strains of *P. aeruginosa* and *A. baumannii*, but also methicillin resistant *Staphylococcus aureus* (MRSA). By profiling with *P. aeruginosa* LPS deletion mutants we show that the added lipid chain is essential to confer activity. **TNS18** apparently acts by a membrane disruptive mechanism, evidenced by the very fast killing kinetics, the formation of disrupted cellular structures visible by transmission electron microscopy (TEM), and vesicle leakage experiments. Circular dichroism (CD) and molecular dynamics (MD) studies suggest that the dendrimer exists in a hydrophobic collapsed conformation in water with its fatty acid chain backfolded onto a hydrophobic pocket formed by the peptide dendrimer branches. We suggest that the dendrimer unfolds in contact with the membrane enabling membrane disruption and rapid bacterial killing. **TNS18** is stable in serum and shows promising activity in a murine infection model with MDR clinical isolates of *A. baumannii* and *E. coli,* providing the first evidence that AMPDs might be amenable to in vivo use.

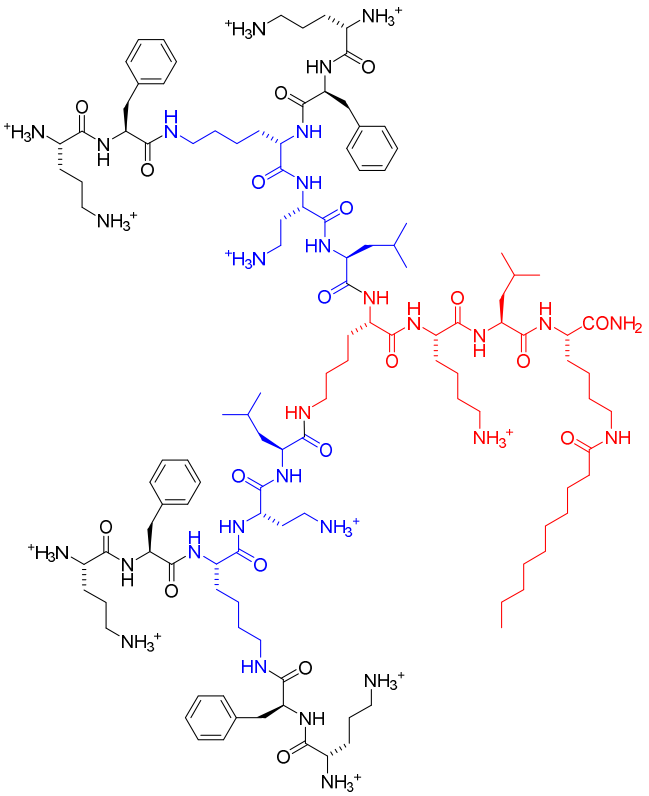

Figure 1. Structure and sequence of G2 AMPD **TNS18**. Residues are colored by dendrimer generation: G0 = red (one copy), G1 = blue (2 copies), G2 = black (4 copies).

Results and Discussion

Lipidation confers antibacterial activity to G2 AMPDs

To obtain lipidated versions of our G2 peptide dendrimer **G2KL** we attached an additional lysine residue at the dendrimer core and acylated its side chain amino group with fatty acids of increasing length. We prepared these dendrimers by solid-phase peptide synthesis (SPPS),[43] which is suitable to prepare a variety of peptide dendrimers,[25] starting with a side chain alloc protected lysine.[44] After completing the G2 branch by coupling of the last four lysine residues, we selectively deprotected the alloc group at the dendrimer core, acylated the resulting free amino group with fatty acids of various chain length (C_6 to C_{24}), and finally removed the four Fmoc groups at the dendrimer periphery and cleaved the dendrimer from the resin and deprotected the remaining Boc-protected lysine side chains by acidic treatment. The procedure provided lipidated dendrimers in pure form and good isolated yields after purification by preparative HPLC (Scheme 1, Table 1).

We tested our lipidated peptide dendrimers for antimicrobial activity against *P. aeruginosa* PAO1 and *Escherichia coli* DH5α as Gram negative and *Bacillus subtilis* BR151 as Gram positive bacterium, as well as for their hemolytic activity on human red blood cells (Table 1). The addition of the side-chain acylated lysine yielded active AMPDs with all acyl chain length tested (C_6 to C_{24}). Elongation of the fatty acid however also led to a gradual increase in hemolysis to the point that hemolysis was even stronger than the antimicrobial effect for C_{18} and C_{24}. From these experiments, we selected the decanoyl group (C_{10}, **TNS03**) as the optimal aliphatic chain length combining good antimicrobial effects on all three test strains with moderate hemolysis.

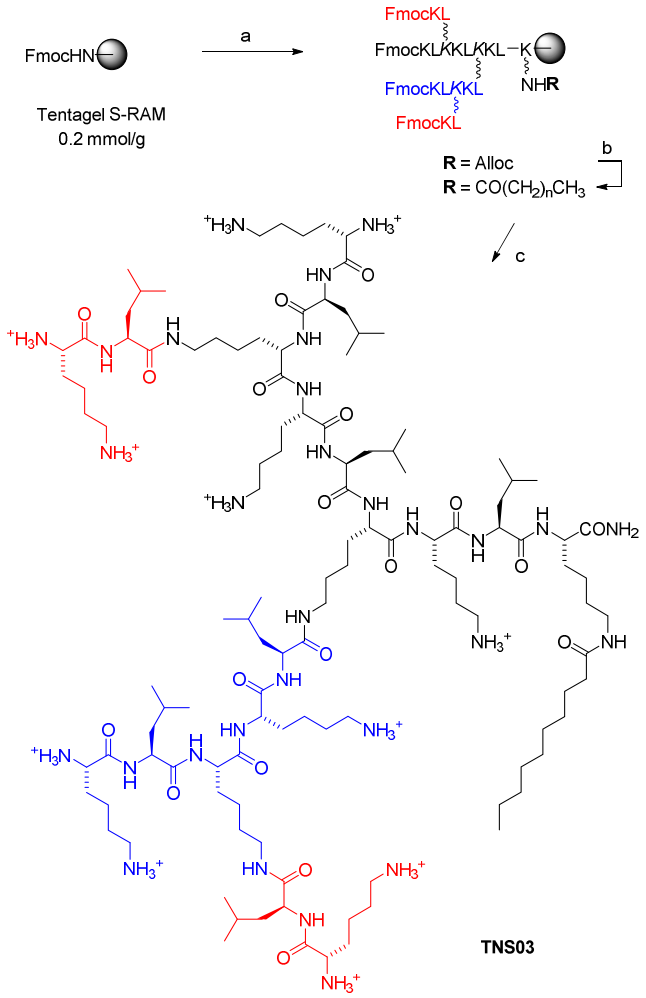

Scheme 1. Synthesis and structure of lipidated peptide dendrimer **TNS03**. Residues are colored by peptide chain: black = main α-peptide chain; blue = peptide chain branched off the G0 side-chain branching; red = peptide chain branched off the G1 side-chain branching. Conditions: a) SPPS; b) $Pd(Ph_3)_4$, $PhSiH_3$, in dry DCM, then decanoic acid, HOBt, DIC, DIPEA; c) 20% piperidine in DMF, then TFA cleavage and HPLC purification.

Table 1. Synthesis and biological activity of AMPDs.

Compound	Sequence[a)]	Yield[b)] mg (%)	MS calc./obs.	*P. aeruginosa*[c)] MIC (μg/mL)	*E. coli*[c)] MIC (μg/mL)	*B. sub.*[c)] MIC (μg/mL)	hRBC[c)] MHC (μg/mL)
G3KL	$(KL)_8(\mathit{K}KL)_4(\mathit{K}KL)_2\mathit{K}KL$	124 (23)	4531.38/4533.38	4	4	3	840
G2KL	$(KL)_4(\mathit{K}KL)_2\mathit{K}KL$	86 (34)	2089.56/2090.57	>64[d]	> 85	> 85	> 1700
TNS01	$(KL)_4(\mathit{K}KL)_2\mathit{K}KLK(C_6)$	23.0 (13)	2315.73/2315.74	16	2	20	1540
TNS02	$(KL)_4(\mathit{K}KL)_2\mathit{K}KLK(C_8)$	27.4 (13)	2343.76/2343.77	4	1	4	1190
TNS03	$(KL)_4(\mathit{K}KL)_2\mathit{K}KLK(C_{10})$	84 (30)	2371.80/2371.80	3	1	2	650
TNS04	$(KL)_4(\mathit{K}KL)_2\mathit{K}KLK(C_{12})$	39.8 (18)	2399.83/2399.83	3	1	2	165
TNS05	$(KL)_4(\mathit{K}KL)_2\mathit{K}KLK(C_{16})$	30.2 (14)	2455.89/2455.90	8	12	nd	11
TNS06	$(KL)_4(\mathit{K}KL)_2\mathit{K}KLK(C_{18})$	52.6 (16)	2483.92/2483.92	9	3	4	2
TNS07	$(KL)_4(\mathit{K}KL)_2\mathit{K}KLK(C_{24})$	56.7 (17)	2568.01/2568.01	54	13	26	1

[a)] One letter code for amino acids. Branching diamino acids in italics. All peptides are carboxamides ($CONH_2$) at the C-terminus. C_n denotes a C_n-fatty acid amidated to the side-chain amino group of Lys in the core. [b)] Yields given for RP-HPLC purified product. [c)] MIC (minimal inhibitory concentration were determined on *P. aeruginosa* PAO1 in Müller-Hinton medium, *Escherichia coli* DH5α in LB medium, and *Bacillus substilis* BR-151 in LB medium, and MHC (minimal hemolytic concentration) determined on human red blood cells (hRBC). Experiments were done in triplicates, values are given in μg/mL and are calculated based on the peptide mass without trifluoroacetate counter ions. nd = not determined. [d)] a MIC value of 7 μg/mL was obtained in LB medium.[31]

Sequence optimization leads to more potent G2 AMPDs

We next optimized the amino acid sequence of **G2KL** focusing on conservative amino acid exchanges in the G1 and G2 branches keeping the alternating hydrophobic and cationic residues motif. We prepared a 1936-member peptide dendrimer library[45] using split-and-mix synthesis with a tentagel resin bearing an acid stable but photolabile linker (Figure 2a).[46, 47] Lysines at X^5 and X^8 were exchanged to ornithine (Orn), diaminobutyric acid (Dab), arginine and histidine, but not lysine to avoid confusion with the branching lysines during the bead decoding step.[45] Leucines X^4 and X^7 were exchanged to phenylalanine, valine, methionine, proline, and leucine itself, as well as to β-alanine (β-Ala), γ-amino butyric acid (GABA) and 4-aminomethyl-benzoic acid (AMBA) to test the effect of dendrimer branch extension on activity. The polar residues threonine, asparagine and glutamate were also included to test if activity might be compatible with these less hydrophobic residues which are also found in naturally occurring AMPs. The library featured a free carboxyl group at the C-terminus liberated by photolysis, which was expected to reduce the antimicrobial effect and facilitate the selection of the most active sequences since the high concentration of peptide around the photolyzed bead might produce an exceedingly high fraction of active beads.

Antimicrobial activity screening was performed by partial photolysis of dried synthesis beads,[46] spreading the beads on an agar plate inoculated with PAO1, incubation at 37°C overnight, staining of live bacteria, and identification of beads surrounded by a clearing zone indicative of antimicrobial activity (Figure 2b).[48] We screened five agar plates, each with 10 mg of library (approx. 10,000 beads), and identified a total of 64 beads with clearing zones (11 beads with large, 28 with medium, 25 with small clearing zones, Table S1), which we picked and subjected to amino acid analysis for sequence determination.[49] Compared to randomly picked beads showing an approximately statistical sequence distribution (Table S2), the most active sequences carried preferentially phenylalanine and leucine at both hydrophobic residue positions X^4 and X^7, diaminobutyric acid at the cationic residue position X^5 within the G1 branch, and ornithine or arginine at the terminal cationic residue position X^8 (Figure 2c). The preference for these residues

was quite strong, with three sequences occurring several times among active beads (15, 14 resp. 7 times). By contrast extended (e.g. β-Ala) or polar (e.g. Thr) residues were not present among the hits, suggesting limited sequence diversity options within this G2 peptide dendrimer architecture.

We resynthesized and tested the three most frequently found sequences together with another five single occurrence hits and two non-hit sequences from beads without any detectable clearing zone (Table 2). While the two non-hit sequences as well as the starting sequence **G2KL** were inactive when tested in MH medium, six of the eight resynthesized G2 dendrimer hits showed activity against PAO1 under these conditions. We selected the three most frequently found hit sequences **TNS08**, **TNS09** and **TNS10** and prepared the corresponding lipidated dendrimers **TNS18**, **TNS19** and **TNS20** as possible improved versions of **TNS03**. Indeed, all three AMPDs displayed excellent activity against PAO1. Although lipidation might enhance protein binding, the antimicrobial activity of our lipidated dendrimers was only slightly reduced in the presence of human serum. We also measured the stability of the various dendrimers towards degradation in human serum (Figure S1). We observed that while **G2KL** ($t_{1/2}$ = 14 h) became slightly more prone to degradation upon lipidation to **TNS03** ($t_{1/2}$ = 8 h), the relatively unstable dendrimer **TNS08** ($t_{1/2}$ = 6 h) was more stable in its lipidated form **TNS18** ($t_{1/2}$ = 20 h), which was as stable as the G3 AMPD **G3KL** ($t_{1/2}$ = 18 h). As observed with **TNS03** the presence of a lipid chain in **TNS18**, **TNS19** and **TNS20** also led to a stronger hemolysis effect compared to the parent non-lipidated dendrimers **TNS08**, **TNS09** and **TNS10**, however the effect was judged acceptable considering the gain in activity obtained by lipidation.

We further profiled our lipidated AMPDs against a broader panel of bacteria comprising four MDR clinical isolates of *P. aeruginosa*, *A. baumannii* 19606, three strains of *E. coli*, and *Stenotrophomonas maltophilia* CP127, all of which belong to problematic Gram-negative pathogens. We also tested *Staphylococcus epidermidis, S. aureus* COL (methicillin resistant) and *S. aureus* Newman (methicillin sensitive) as Gram positive bacteria (Table 3). Remarkably, our sequence optimized lipidated G2 AMPDs were not only more active than the previous best and

much larger AMPD **G3KL** or the starting sequence **TNS03**, but for the first time they were now also active against Gram positive bacteria including MRSA, against which polymyxin or **G3KL** or **TNS03** were inactive. **TNS18** with ornithine (X^8), phenylalanine (X^7), diaminobutyric acid (X^5) and leucine (X^4) stood out as the most active AMPD in the series.

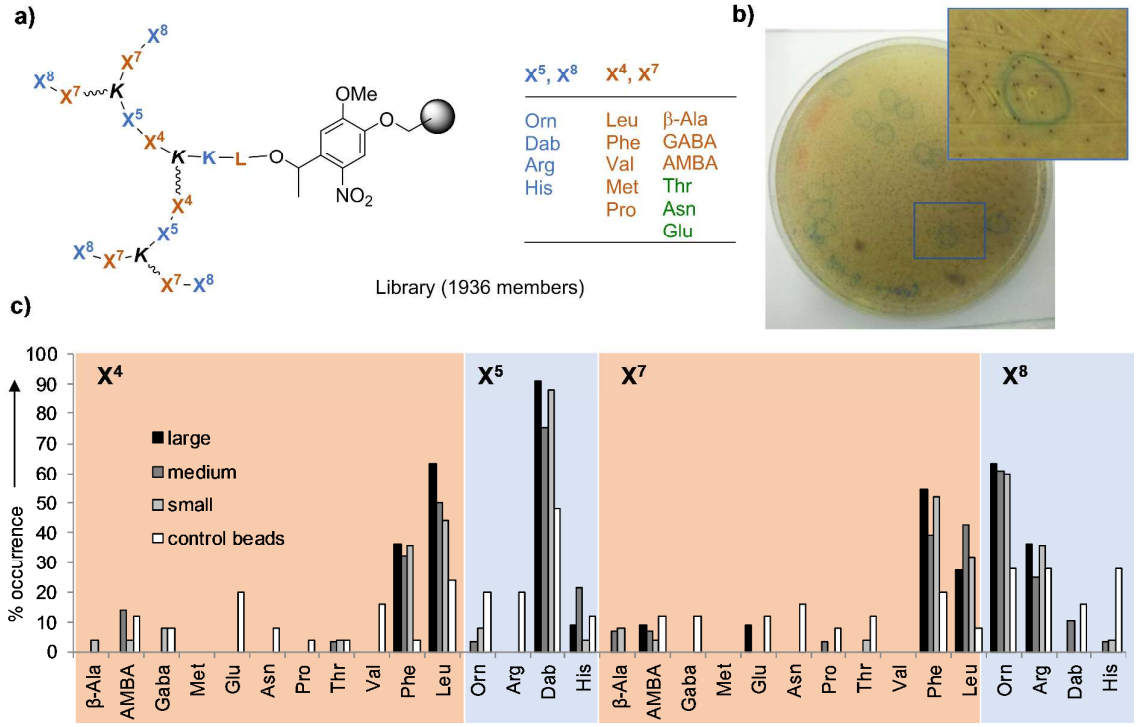

Figure 2. Optimization of the **G2KL** peptide dendrimer sequence. **(a)** Structure and sequence composition of the 1936-member combinatorial peptide dendrimer library. **(b)** PAO1 antimicrobial activity screening on agar plates inoculated with PAO1. After addition of dried photolyzed bead the plates were incubated at 37°C overnight and stained for live bacteria with MTT. Beads surrounded by a clearing zone indicative of antimicrobial activity are highlighted. **(c)** Amino acid composition of dendrimers in beads with large, medium or small clearing zone, and of control beads picked randomly before photolysis. Sequences of all beads analyzed are given in Table S1 and S2.

Table 2. Synthesis and activity of reference compounds, library hits, non-hits, and selected lipidated hits.

Compound	Sequence[a]	No. of hits[b]	Yield mg (%)[c]	MS calc./obs.[d]	PAO1 MIC[e] (μg/mL) MH	PAO1 MIC[e] (μg/mL) + serum	serum $t_{1/2}$[f]	hRBC MHC[g] (μg/mL)
Polymyxin B	Cyclic peptide	-	-	-	2-4			>2000
G3KL	$(KL)_8(KKL)_4(KKL)_2KKL$	-	124 (23)	4531.38/4533.38	4	4	18 h	1000
G2KL	$(KL)_4(KKL)_2KKL$	-	86 (34)	2089.56/2090.57	>128	>128	14 h	>2000
TNS03	$(KL)_4(KKL)_2KKLK(C_{10})$	-	84 (30)	2371.80/2372.79	4	8	8 h	1000
Library Hits:								
TNS08	$(OF)_4(KBL)_2KKL$	15	44 (17)	2113.38/2113.38	32	32	6 h	>2000
TNS09	$(OL)_4(KBF)_2KKL$	14	30 (22)	2045.41/2045.41	>128	>128		>2000
TNS10	$(RF)_4(KBL)_2KKL$	7	44 (13)	2281.46/2281.47	16	32		>2000
TNS11	$(OF)_4(KB\beta A)_2KKL$	1	38 (16)	2029.28/2029.28	>128			>2000
TNS12	$(BL)_4(KBL)_2KKL$	1	28 (12)	1921.37/1921.37	128			1000
TNS13	$(RX)_4(KBF)_2KKL$	1	28 (15)	2293.37/2293.37	64			
TNS14	$(RE)_4(KBL)_2KKL$	1	32 (14)	2209.36 /2209.36	>128			1000
TNS15	$(RL)_4(KHF)_2KKL$	1	42 (12)	2287.49/2287.49	128			>2000
Non-hits:								
TNS16	$(BT)_4(KRL)_2KKL$	-	36 (11)	1985.30/1985.31	>128			
TNS17	$(OZ)_4(KHV)_2KKL$	-	12 (5)	1911.27/1911.28	>128			>2000
Lipidated hits:								
TNS18	$(OF)_4(KBL)_2KKLK(C_{10})$	-	121 (42)	2395.61/2395.61	2	8	20 h	500
TNS19	$(OL)_4(KBF)_2KKLK(C_{10})$	-	28 (9)	2327.64/2327.64	2	8	24 h	500
TNS20	$(RF)_4(KBL)_2KKLK(C_{10})$	-	24 (11)	2563.69/2563.70	4-8	16	18 h	500

[a] One-letter codes for amino acids, O = ornithine, X = 4-aminomethyl-benzoic acid, Z = γ-aminobutyric acid, B = diaminobutyric acid, *K* = branching lysine, βA = β-alanine, $K(C_{10})$ = side-chain decanoylated lysine. C-termini are carboxamide $CONH_2$. [b] number of times the sequence was found on beads marked as active in agar plate screening. [c] Yields given for RP-HPLC purified product. [d] High resolution electrospray ionization mass spectrometry (positive mode), the calculated monoisotopic mass and the observed mass in the reconstructed spectrum are given. [e] MIC (minimal inhibitory concentration) were determined on *P. aeruginosa* PAO1 in Müller-Hinton medium, with or without 30% v/v human serum. [f] half-life for degradation in human serum as determined by analytical HPLC, see methods for details. [g] MHC (minimal hemolytic concentration) determined on human red blood cells (hRBC). Experiments were done in triplicates, values are given in μg/mL and are calculated based on the peptide mass without trifluoroacetate counter ions. Missing entries were not determined.

Table 3. Activity of AMPDs against multidrug resistant clinical isolates of *P. aeruginosa* and other bacteria strains.[a]

	Polymxin B	**G3KL**	**TNS03**	**TNS18**	**TNS19**	**TNS20**
MDR *P. aeruginosa*						
ZEM-9A	8	32-64	16-8	8	8	16-32
ZEM-1A	<1	4	4	4	4	4-8
PEJ9.1	2	64	64	32	>64	32
PEJ2.6	1	16	8	4	16	8
Gram negative bacteria						
A.baumannii 19606	<1	8-16	16	8-16	32	8-16
E. coli (CP46)	<0.5	>64	32	8	n.d.	8-4
E. coli W3110 (TE823)	<0.5	8	4	4	n.d.	4
E. coli MG1665 (TE824)	<0.5	8	4	4	n.d.	4
St. maltophilia (CP127)	>64	64	64	16	n.d.	16
Gram positive bacteria						
S.epidermidis	64	2	2	2	2	2
S.aureus COL	64	>64	64	8-16	32-64	8
S.aureus Newman	>64	>64	64	16	n.d.	8

[a] Minimal inhibitory concentrations (MIC) given in μg/mL were determined in Müller-Hinton medium. Experiments were done in triplicates. Values are calculated based on the peptide mass without trifluoroacetate counter ions. n.d. = not determined.

G2 dendrimers require the core lipid chain to pass the LPS layer

To better understand the role of the lipid chain in the activity of **TNS18** and analogs we profiled our G2 dendrimers against wild-type PAO1, a PAO1*rmd* mutant (PT1482) lacking the A-band lipopolysaccharide (LPS) composed of D-rhamnose trisaccharides, and a PAO1*rmlC* mutant (PT1495) lacking both A- and B-band of the LPS.[50] The non-lipidated G2 dendrimers such as **TNS08** were all inactive against PAO1 and PAO1*rmd* (PT1482), but showed good activity against PAO1*rmlC* (PT1495) lacking both A- and B-band LPS components (Table 4). By contrast, **TNS18** and related lipidated G2 dendrimers were active on all variants independent of the LPS composition of the bacterial outer membrane, similarly to polymyxin B and our previous G3 dendrimer **G3KL**. This data indicated that the core fatty acid on G2 dendrimers is required for passing the LPS layer, which is similar to the reported effect of the N-terminal fatty acid appendage of polymyxin B.[36]

Table 4. Antimicrobial activity of AMPDs against PAO1 and LPS deletion mutants of *P. aeruginosa*.

AMPD	PAO1	PAO1*rmd* (A-)	PAO1*rmlC* (A-B-)
Polymyxin B	1	1	<1
G2KL	>64	>64	16
G3KL	4	4	4
TNS02	10	10	5
TNS03	8	4	4
TNS04	5	5	4
TNS08	>64	>64	4
TNS09	>64	>64	8
TNS10	>64	64	4
TNS18	4	4	2-4
TNS19	4-8	4	4
TNS20	8	8	4

MIC (μg/mL) was determined in MH-medium on a 96 well plate and incubation overnight (18-22 hours) at 37°C. Maximal measured concentration is 64 μg/mL. Each AMPD was measured in two independent duplicates.

Lipidated AMPDs disrupt bacterial membranes

Time-kill experiments showed complete killing of PAO1 within 30 min of incubation with **TNS18**, which was slightly faster than for **TNS03** (1h), polymyxin B and **G3KL** (2h), or tobramycin (3h) (Figure 3). Rapid killing is often indicative of a membrane disruptive mechanism of action.[51] Analysis by transmission electron microscopy (TEM) showed that treating PAO1 cells with polymyxin B (10×MIC, 5 μg/mL) for 15-60 min produced characteristic protrusions in the outer membrane of PAO1, reproducing earlier reports,[52] while control cells were unaffected. Under the same conditions AMPDs **TNS03** and **TNS18** (10×MIC, 40 μg/mL) produced even more significant membrane perturbations leading to emptying of the cell content (Figure 4a, Figure S2). Similar effects were observed with the larger AMPD **G3KL**, suggesting a similar mechanism for G2 and G3 dendrimers. On the other hand, the non-lipidated dendrimer **G2KL** only produced a very weak effect, and this only at a much higher concentration (128 μg/mL), in line with its very weak activity.

The membrane disruptive activity of our lipidated G2 dendrimers was further evidenced by vesicle leakage experiments with large unilamellar vesicles (LUVs). Treating fluorescein loaded LUVs consisting of the anionic lipid phosphatidyl glycerol mimicking the bacterial membrane with Polymyxin B led to fluorescein release as evidence for membrane perturbation (Figure 4b). Dendrimers **TNS03**, **TNS18** and **G3KL** produced a similar effect, but with somewhat faster kinetics of release, while **G2KL** lacking the lipid chain was less and slower acting. By contrast LUVs consisting of the zwitterionic lipid phosphatidyl ethanolamine mimicking the eukaryotic membrane were only weakly affected by these compounds, in line with their relatively modest hemolytic activity (Figure 4c).

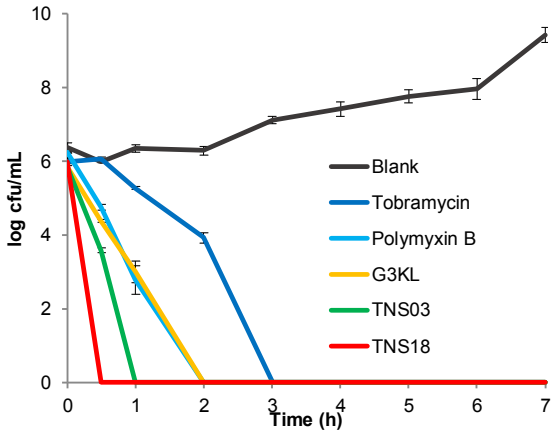

Figure 3. Time-kill assay showed *P. aeruginosa* bacteria cell death at 37°C in MH medium measured at 2×MIC for Tobramycin (0.5 μg/mL), Polymyxin B (0.5 μg/mL), **G3KL** (8 μg/mL), **TNS03** (8 μg/mL), and **TNS18** (8 μg/mL).

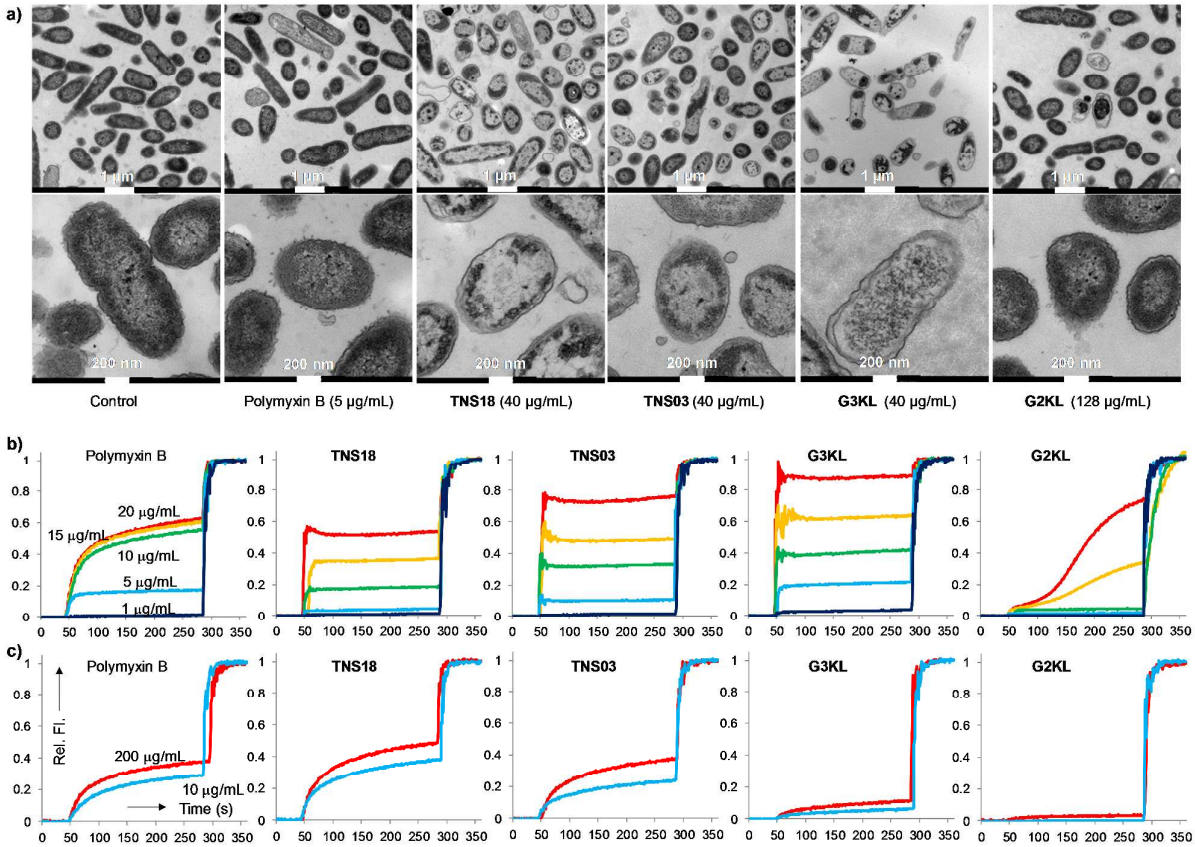

Figure 4. Membrane disruptive properties of AMPDs. **(a)** TEM images of *P. aeruginosa* cells treated for 60 min. at 10×MIC with Polymyxin B (5 μg/mL), **TNS18** (40 μg/mL), **TNS03** (40 μg/mL), and **G3KL** (40 μg/mL) and **G2KL** (128 μg/mL). Enlarged TEM images are shown in Figure S2. **(b)** Fluorescein leakage assay from phosphatidyl glycerol LUVs. **(c)** Fluorescein leakage assay from phosphatidyl choline LUVs. LUVs were suspended in buffer (10 mM TRIS, 107 mM NaCl, pH 7.4). After 50 sec the indicated compound was added to reach the indicated concentration. After 300 sec 1.2% Triton X-100 was added for full fluorescein release.

Spectroscopic studies

Diffusion NMR showed hydrodynamic radii expected for a monomeric state in aqueous buffer at different pH and in the presence of trifluoroethanol (TFE) (Figure S3, Table S3). Furthermore we did not detect any micelle formation up to 10 mg/mL using the Nile Red assay,[53] excluding micelle formation as a possible explanation for antimicrobial activity (Figure S4).

Many linear AMPs undergo a conformational transition in contact with the bacterial membrane leading to the formation of a membrane disruptive amphiphilic structure,[4-8] which is most often an α-helix observable by circular dichroism (CD) in aqueous buffer upon addition of 20% v/v TFE.[54] Here we found that **TNS03** (Figure 5a), and to a lower extent **G2KL** (Figure 5b), behaved similarity to linear α-helical AMPs by showing a typical random coil signal in neutral aqueous buffer with transition to an α-helical signal upon addition of 20% v/v TFE, a situation observed previously with AMPD **G3KL** which has a similar sequence.[31] **TNS18** behaved similarly, although its CD signals in water and in the presence of TFE did not resemble the CD signature of linear random coils and α-helices as perfectly as those of **TNS03** (Figure 5c). Its non-lipidated analog **TNS08** showed a similar but also rather weak CD signal transition upon addition of TFE (Figure 5d).

Taken together, these spectroscopic studies showed that **TNS18** and related G2 AMPDs were not aggregating in water, but underwent a conformational transition to an α-helix like conformation when exposed to TFE similarly to typical AMPs.

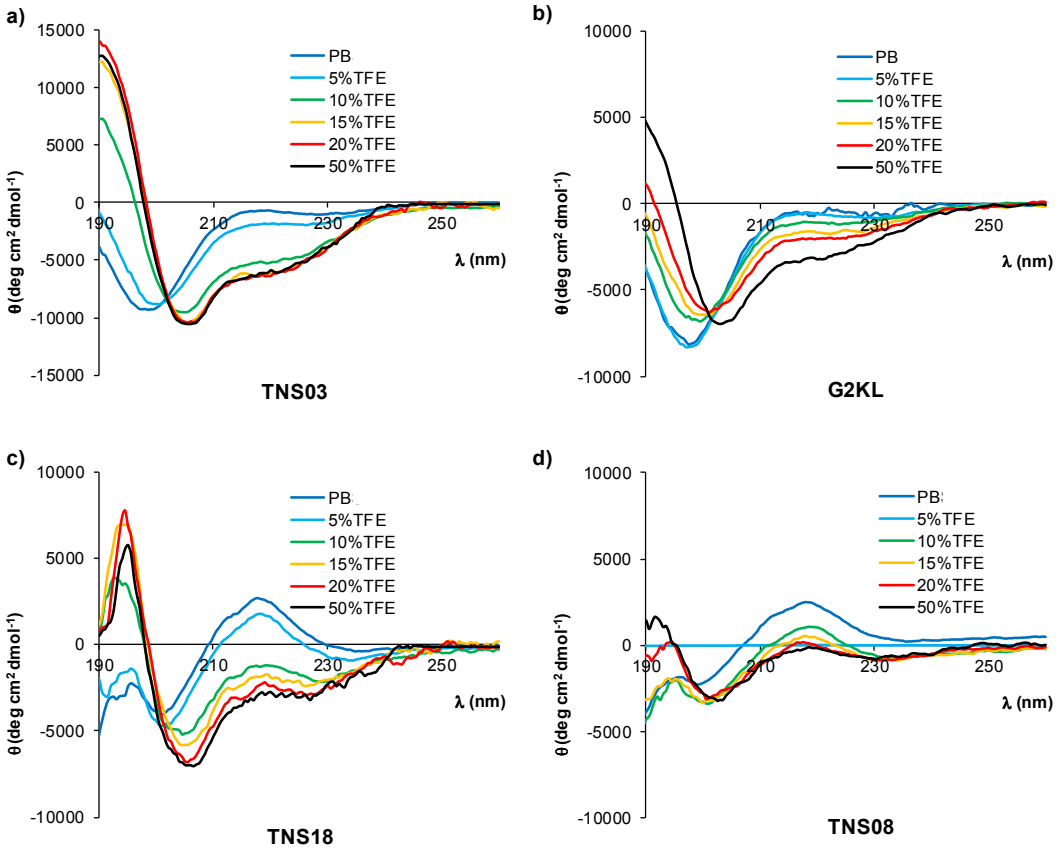

Figure 5. CD spectra of AMPDs (200 μg/mL) in 8 mM aqueous phosphate buffer pH 7.4 (PB) with increasing percentage of trifluoroethanol (TFE). **(a) TNS03**. **(b) G2KL**. **(c) TNS18**. **(d) TNS08**.

Molecular modelling

The α-helical CD signals observed with our dendrimers in the presence of TFE might be explained by folding of the linear α-nonapeptide present along the α-peptide backbone of the dendrimer (Scheme 1) into a standard α-helix as observed previously with G2 peptide dendrimers designed to include an α-helix in their structure.[55] To test this hypothesis, we built the corresponding structural models for our most active AMPD **TNS18** and its analog **TNS03**, and performed molecular dynamics (MD) simulations over 500 ns at 300 K in water with or without 20% TFE using the GROMACS molecular modeling package.[56]

Both dendrimers rapidly unfolded in pure water, but their α-helical structures were partly stabilized in the presence of 20% TFE, in line with the CD data (Figure 6a and Figure S5a). The

helix stabilization effect with 20% TFE was most pronounced with **TNS18**, whose central α-peptide chain retained its α-helical conformation over the course of the entire simulation. A snapshot of the dendrimer after 100 ns showed an extended fatty acid and hydrophobic residues exposed to the solvent, which might correspond to the conformation of the dendrimer within the membrane environment (Figure 6b/e). In the case of **TNS03** the initial α-helical folding of the central α-peptide chain was only partially preserved during the first 200 ns of the simulation. In this case the snapshot at 100 ns showed a hydrophobically collapsed state with a backfolded fatty acid chain and cationic residues exposed to the solvent, as expected for a conformation in water (Figure S5b/c).

To test if a hydrophobically collapsed structure might also exist for **TNS18** in water, we equilibrated its structure by MD at 450 K, and performed 10 parallel cooling cycles from 10 different starting high energy conformations sampled at 450 K. Seven out of ten trajectories converged to a consistently compact conformation at 300 K. This structure showed a β-sheet like pattern involving up to five backbone H-bonds connecting the main α-peptide branch spanning from G0 through G2 with one each of the G1 and G2 dipeptides (Figure 6c). This β-sheet like conformation, which might explain the somewhat unusual CD signal of **TNS18**, was also reflected in the Ramachandran plot, where 73 % of the (ϕ, φ)-angles resided in the β-sheet region (Figure 6d). In this conformation the lipid chain at the dendrimer core is backfolded onto the peptide dendrimer branches forming a hydrophobic pocket, resulting in hydrophobically collapsed globular structure exposing cationic residues on the outside (Figure 6f). This structure can be interpreted as the non-aggregating conformation of the dendrimer in water.

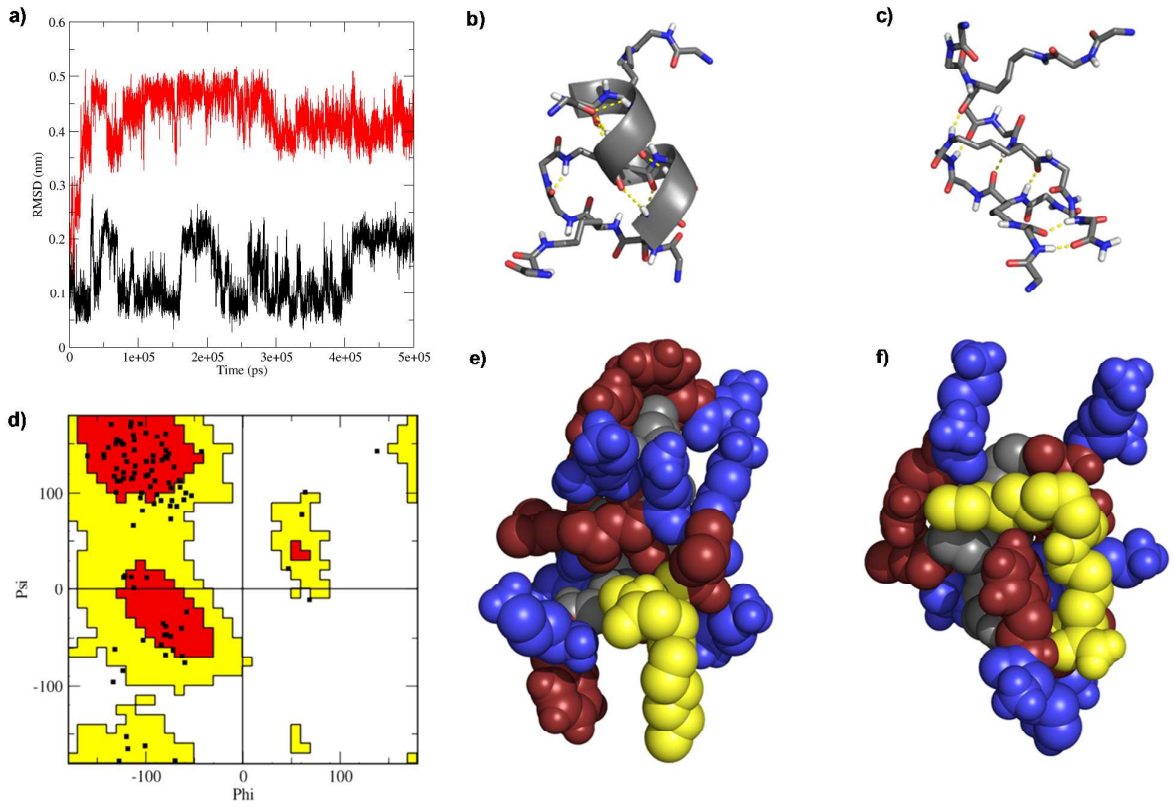

Figure 6. Molecular dynamics simulation of AMPD **TNS18**. **(a)** MD trajectory of **TNS18** as RMSD plot of the central helix from the starting fully α-helical conformation in water (red line) and with 20% TFE in water (black line). **(b)** stick model of the backbone of **TNS18** after 100 ns in an α-helical conformation. **(c)** Stick model of the minimized, hydrophobically collapsed β-sheet like structure of **TNS18** in water after simulated annealing and clustering. **(d)** Ramachandran plot of peptide bond angles in the structures of **TNS18** at 300 K from 7 independent simulated annealing MD runs. **(e)** CPK model of the structure shown in (b). **(f)** CPK model of the structure shown in (c).

Mechanistic hypothesis

The experiments and modeling studies above suggest a possible mechanism of action in which dendrimer **TNS18** exists in a hydrophobically collapsed β-sheet like conformation in water (Figure 5c and Figure 6c/f) explaining the observed good water solubility and absence of aggregation. This folded conformation should persist when the dendrimer traverses the relatively polar LPS layer, and unfold in contact with the membrane to an extended and possibly α-helical conformation (Figure 6b/e) exposing its lipid chain and hydrophobic side chains and enabling interaction with membrane lipids, leading to accumulation and eventually membrane perturbation and bacterial killing (Figures 3 and 4).

The MD simulations suggest that the stronger antibacterial activity of the sequence optimized **TNS18** compared to its parent dendrimer **TNS03** might reflect stronger stabilization of the extended and membrane disruptive conformation compared to the hydrophobically collapsed state. The data with LPS mutant strains (Table 4) suggest that the non-lipidated dendrimers **TNS08** and **G2KL** remain in the LPS layer and cannot accumulate in the membrane by lack of a lipid appendage, explaining their lower activity. In the case of **G3KL**, its larger size and number of positive charges (23+) compared to G2 dendrimers (9+) probably allows binding interactions with the negatively charged lipid A and membrane accumulation even without a lipid chain. It should be noted that our dendrimers do not seem to form amphiphilic conformations segregating cationic and hydrophobic residues in two groups as often observed with linear α-helical AMPs, suggesting that membrane perturbation might occur via the "carpet" model rather than by pore formation.[5]

In vivo activity

To test if our dendrimers might be used in vivo we carried out a preliminary study in a mouse infection model. We considered our best lipidated G2 dendrimer **TNS18** as well as our earlier **G3KL**, which had not been previously tested in vivo. Both dendrimers were converted from their trifluoroacetate salt to acetate salt by ion exchange for in vivo studies.[57] In this model, we used an MDR *A. baumannii* strain abaX1605034 (Table S4), which was sensitive in vitro to Polymyxin B (MIC = 1-2 μg/mL) as well as to both AMPDs (MIC = 4-8 μg/mL).

BALB/c mice were infected intraperitoneally with 1.6×10^8 CFU bacterial cells, and treated with three successive injections (t = 0 h, 8 h, 16 h) of 5 mg/kg AMPD, polymyxin, or saline as a control. While all but one mice died within 15 h when left untreated, mice treated with **TNS18** showed complete survival, which was comparable to the effect with polymyxin B (Figure 7a). On the other hand our previously reported G3 dendrimer **G3KL** was ineffective in this *in vivo* infection model. Non-infected mice treated with the same amounts of **G3KL** of **TNS18** were entirely unaffected, showing that the dendrimers were not toxic by themselves. In a second series of

experiments we also tested **TNS18** to treat mice intraperitoneally infected by a MDR *Escherichia coli* strain and similarly observed 100% survival of treated animals. By comparison imipenem, to which the strain is sensitive, only provided partial protection, and ceftriaxone, to which the strain is resistant, was even less effective (Figure 7b).

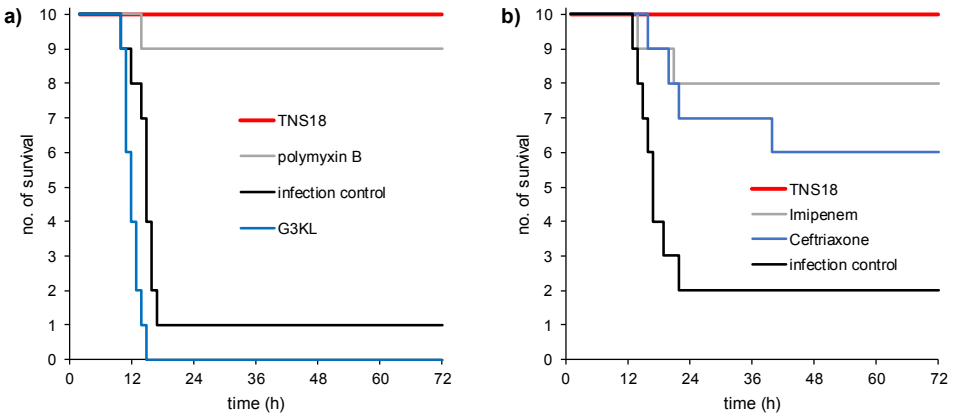

Figure 7. In vivo activity of AMPDs. **(a)** Survival of mice over time infected by MDR *A. baumannii* strain abaX1605034 (0.5 mL of 3.2×10^8 CFU/mL) and treated with 3 x 5 mg/kg Polymyxin B or AMPD (0h, 8h, 16h). **(b)** Survival of mice over time infected by MDR *E. coli* strain *SP1708* (0.5 mL of 3.5×10^8 CFU/mL) and treated with **TNS18** (3 × 5 mg/kg, MIC = 8 µg/mL), Ceftriaxone (3 x 5 mg/kg, MIC > 64 µg/mL) or imipenem (3 × 0.2 mg/kg, MIC < 1 µg/mL).

Conclusion

The experiments above show that lipidated G2 peptide dendrimer **TNS18** exerts potent antimicrobial effects against MDR Gram negative bacteria such as *P. aeruginosa*, *A. baumannii* and *E. coli,* as well as against Gram positive bacteria such as MRSA, for which **G3KL**, **TNS03** or the reference antibiotic polymyxin B are inactive. Profiling with *P. aeruginosa* LPS deletion mutants show that the presence of the lipid chain is essential to enable penetration of the lipopolysaccharide layer. The very rapid killing kinetics, the induction of membrane punctures and emptying of cell contents visible by TEM, and direct interactions with bacterial membrane lipids in vesicle leakage experiments with LUVs, indicate that our dendrimer exert potent membrane perturbation effects of bacteria. Spectroscopic studies combined with MD simulations suggest that **TNS18** adopts a hydrophobically collapsed β-sheet like conformation in water with its lipid chain backfolded onto the peptide dendrimer. As a possible mechanism of action against Gram-negative bacteria, we propose that the dendrimer traverses the LPS layer in this hydrophobically collapsed conformation, and then unfolds in contact with the membrane to form an α-helical like conformation exposing its hydrophobic side chains and fatty acid, thereby enabling accumulation and membrane perturbation. A preliminary in vivo study with a murine infection model using MDR *A. baumannii* and *E. coli* clinical isolates shows promising activities for **TNS18**. Taken together, these data suggest that lipidated G2 AMPDs might be promising candidates for further development as new antimicrobial agents.

Methods

Synthesis and characterization of peptide dendrimers and all assays, measurements, and modeling studies are described in the supporting information.

Supporting information. Details of synthesis and characterization of peptide dendrimers and all assays, measurements, and modeling studies. This information is available free of charge at http://pubs.acs.org.

Acknowledgements. This work was supported financially by the Swiss National Science Foundation (Grants no. 200020159941, IZLCZ2155982 and NRP72) and the Swiss TransMed (B5 platform project).

References

1. O'Connell, K. M. G.; Hodgkinson, J. T.; Sore, H. F.; Welch, M.; Salmond, G. P. C.; Spring, D. R. *Angew. Chem., Int. Ed. Engl.* **2013,** *52*, 10706-10733.

2. Tommasi, R.; Brown, D. G.; Walkup, G. K.; Manchester, J. I.; Miller, A. A. *Nat. Rev. Drug Discovery* **2015,** *14*, 529-542.

3. Fleeman, R.; LaVoi, T. M.; Santos, R. G.; Morales, A.; Nefzi, A.; Welmaker, G. S.; Medina-Franco, J. L.; Giulianotti, M. A.; Houghten, R. A.; Shaw, L. N. *J. Med. Chem.* **2015,** *58*, 3340-3355.

4. Zasloff, M. *Nature* **2002,** *415*, 389-395.

5. Nguyen, L. T.; Haney, E. F.; Vogel, H. J. *Trends in Biotechnology* **2011,** *29*, 464-472.

6. Cotter, P. D.; Ross, R. P.; Hill, C. *Nature Reviews Microbiology* **2013,** *11*, 95-105.

7. Fox, J. L. *Nat. Biotech.* **2013,** *31*, 379-382.

8. Mojsoska, B.; Jenssen, H. *Pharmaceuticals (Basel)* **2015,** *8*, 366-415.

9. Fletcher, J. T.; Finlay, J. A.; Callow, M. E.; Callow, J. A.; Ghadiri, M. R. *Chem. Eur. J.* **2007,** *13*, 4008-4013.

10. Hayouka, Z.; Chakraborty, S.; Liu, R.; Boersma, M. D.; Weisblum, B.; Gellman, S. H. *J. Am. Chem. Soc.* **2013,** *135*, 11748-11751.

11. Lichtenecker, R. J.; Ellinger, B.; Han, H. M.; Jadhav, K. B.; Baumann, S.; Makarewicz, O.; Grabenbauer, M.; Arndt, H. D. *Chembiochem* **2013,** *14*, 2492-2499.

12. Hayouka, Z.; Bella, A.; Stern, T.; Ray, S.; Jiang, H.; Grovenor, C. R. M.; Ryadnov, M. G. *Angew. Chem., Int. Ed. Engl.* **2017,** *56*, 8099-8103.

13. Horne, W. S.; Gellman, S. H. *Acc. Chem. Res.* **2008,** *41*, 1399-1408.

14. Fowler, S. A.; Blackwell, H. E. *Org. Biomol. Chem.* **2009,** *7*, 1508-1524.

15. Dohm, M. T.; Kapoor, R.; Barron, A. E. *Curr. Pharm. Des.* **2011,** *17*, 2732-2747.

16. Chongsiriwatana, N. P.; Wetzler, M.; Barron, A. E. *Antimicrob. Agents Chemother.* **2011,** *55*, 5399-5402.

17. Chongsiriwatana, N. P.; Miller, T. M.; Wetzler, M.; Vakulenko, S.; Karlsson, A. J.; Palecek, S. P.; Mobashery, S.; Barron, A. E. *Antimicrob. Agents Chemother.* **2011,** *55*, 417-420.

18. Huang, M. L.; Benson, M. A.; Shin, S. B. Y.; Torres, V. J.; Kirshenbaum, K. *Eur. J. Org. Chem.* **2013,** *2013*, 3560-3566.

19. Eggimann, G. A.; Bolt, H. L.; Denny, P. W.; Cobb, S. L. *ChemMedChem* **2015,** *10*, 233-237.

20. Czyzewski, A. M.; Jenssen, H.; Fjell, C. D.; Waldbrook, M.; Chongsiriwatana, N. P.; Yuen, E.; Hancock, R. E.; Barron, A. E. *PLoS One* **2016,** *11*, e0135961.

21. Liu, R.; Chen, X.; Falk, S. P.; Mowery, B. P.; Karlsson, A. J.; Weisblum, B.; Palecek, S. P.; Masters, K. S.; Gellman, S. H. *J. Am. Chem. Soc.* **2014,** *136*, 4333-4342.

22. Choi, H.; Chakraborty, S.; Liu, R.; Gellman, S. H.; Weisshaar, J. C. *ACS Chem. Biol.* **2016,** *11*, 113-120.

23. Claudon, P.; Violette, A.; Lamour, K.; Decossas, M.; Fournel, S.; Heurtault, B.; Godet, J.; Mely, Y.; Jamart-Gregoire, B.; Averlant-Petit, M. C.; Briand, J. P.; Duportail, G.; Monteil, H.; Guichard, G. *Angew. Chem., Int. Ed. Engl.* **2010,** *49*, 333-336.

24. Teyssières, E.; Corre, J.-P.; Antunes, S.; Rougeot, C.; Dugave, C.; Jouvion, G.; Claudon, P.; Mikaty, G.; Douat, C.; Goossens, P. L.; Guichard, G. *J. Med. Chem.* **2016,** *59*, 8221-8232.

25. Reymond, J.-L.; Darbre, T. *Org. Biomol. Chem.* **2012,** *10*, 1483-1492.

26. Reymond, J. L.; Darbre, T. *Chimia* **2013,** *67*, 864-867.

27. Di Bonaventura, I.; Jin, X.; Visini, R.; Probst, D.; Javor, S.; Gan, B.-H.; Michaud, G.; Natalello, A.; Doglia, S. M.; Kohler, T.; van Delden, C.; Stocker, A.; Darbre, T.; Reymond, J.-L. *Chem. Sci.* **2017,** *8*, 6784-6798.

28. Tam, J. P.; Lu, Y. A.; Yang, J. L. *Eur. J. Biochem.* **2002,** *269*, 923-932.

29. Young, A. W.; Liu, Z.; Zhou, C.; Totsingan, F.; Jiwrajka, N.; Shi, Z.; Kallenbach, N. R. *Medchemcomm* **2011,** *2*, 308-314.

30. Mintzer, M. A.; Dane, E. L.; O'Toole, G. A.; Grinstaff, M. W. *Mol. Pharm.* **2012,** *9*, 342-354.

31. Stach, M.; Siriwardena, T. N.; Kohler, T.; van Delden, C.; Darbre, T.; Reymond, J. L. *Angew. Chem., Int. Ed. Engl.* **2014,** *53*, 12827-12831.

32. Pires, J.; Siriwardena, T. N.; Stach, M.; Tinguely, R.; Kasraian, S.; Luzzaro, F.; Leib, S. L.; Darbre, T.; Reymond, J. L.; Endimiani, A. *Antimicrob. Agents Chemother.* **2015,** *59*, 7915-7918.

33. Abdel-Sayed, P.; Kaeppeli, A.; Siriwardena, T.; Darbre, T.; Perron, K.; Jafari, P.; Reymond, J.-L.; Pioletti, D. P.; Applegate, L. A. *Sci. Rep.* **2016,** *6*, 22020.

34. Cochrane, S. A.; Lohans, C. T.; Brandelli, J. R.; Mulvey, G.; Armstrong, G. D.; Vederas, J. C. *J. Med. Chem.* **2014,** *57*, 1127-1131.

35. Koh, J. J.; Lin, H.; Caroline, V.; Chew, Y. S.; Pang, L. M.; Aung, T. T.; Li, J.; Lakshminarayanan, R.; Tan, D. T.; Verma, C.; Tan, A. L.; Beuerman, R. W.; Liu, S. *J. Med. Chem.* **2015,** *58*, 6533-6548.

36. Velkov, T.; Thompson, P. E.; Nation, R. L.; Li, J. *J. Med. Chem.* **2010,** *53*, 1898-1916.

37. Gallardo-Godoy, A.; Muldoon, C.; Becker, B.; Elliott, A. G.; Lash, L. H.; Huang, J. X.; Butler, M. S.; Pelingon, R.; Kavanagh, A. M.; Ramu, S.; Phetsang, W.; Blaskovich, M. A. T.; Cooper, M. A. *J. Med. Chem.* **2016,** *59*, 1068-1077.

38. Liu, Y. Y.; Wang, Y.; Walsh, T. R.; Yi, L. X.; Zhang, R.; Spencer, J.; Doi, Y.; Tian, G.; Dong, B.; Huang, X.; Yu, L. F.; Gu, D.; Ren, H.; Chen, X.; Lv, L.; He, D.; Zhou, H.; Liang, Z.; Liu, J. H.; Shen, J. *Lancet Infect. Dis.* **2016,** *16*, 161-168.

39. Nordmann, P.; Poirel, L. *Clin. Microbiol. Infect.* **2016,** *22*, 398-400.

40. Kratz, F. *J. Control. Release* **2008,** *132*, 171-183.

41. Kurtzhals, P.; Havelund, S.; Jonassen, I.; Markussen, J. *J. Pharm. Sci.* **1997,** *86*, 1365-1368.

42. Li, Y.; Wang, Y.; Wei, Q.; Zheng, X.; Tang, L.; Kong, D.; Gong, M. *Sci. Rep.* **2015,** *5*, 18039.

43. Amblard, M.; Fehrentz, J. A.; Martinez, J.; Subra, G. *Mol. Biotechnol.* **2006,** *33*, 239-254.

44. Eggimann, G. A.; Blattes, E.; Buschor, S.; Biswas, R.; Kammer, S. M.; Darbre, T.; Reymond, J. L. *Chem. Commun.* **2014,** *50*, 7254-7257.

45. Clouet, A.; Darbre, T.; Reymond, J. L. *Angew. Chem., Int. Ed.* **2004,** *43*, 4612-4615.

46. Maillard, N.; Darbre, T.; Reymond, J. L. *J. Comb. Chem.* **2009,** *11*, 667-675.

47. Stach, M.; Maillard, N.; Kadam, R. U.; Kalbermatter, D.; Meury, M.; Page, M. G. P.; Fotiadis, D.; Darbre, T.; Reymond, J.-L. *MedChemComm* **2012,** *3*, 86-89.

48. Fluxa, V. S.; Maillard, N.; Page, M. G.; Reymond, J. L. *Chem. Commun.* **2011,** *47*, 1434-1436.

49. Kofoed, J.; Reymond, J. L. *J Comb Chem* **2007,** *9*, 1046-52.

50. Köhler, T.; Donner, V.; van Delden, C. *J. Bacteriol.* **2010,** *192*, 1921-1928.

51. Srinivas, N.; Jetter, P.; Ueberbacher, B. J.; Werneburg, M.; Zerbe, K.; Steinmann, J.; Van der Meijden, B.; Bernardini, F.; Lederer, A.; Dias, R. L. A.; Misson, P. E.; Henze, H.; Zumbrunn, J.; Gombert, F. O.; Obrecht, D.; Hunziker, P.; Schauer, S.; Ziegler, U.; Kach, A.; Eberl, L.; Riedel, K.; DeMarco, S. J.; Robinson, J. A. *Science* **2010,** *327*, 1010-1013.

52. Koike, M.; Iida, K.; Matsuo, T. *J. Bacteriol.* **1969,** *97*, 448-452.

53. Stuart, M. C. A.; van de Pas, J. C.; Engberts, J. B. F. N. *J. Phys. Org. Chem.* **2005,** *18*, 929-934.

54. Arunkumar, A. I.; Kumar, T. K.; Yu, C. *Int. J. Biol. Macromol.* **1997,** *21*, 223-230.

55. Javor, S.; Natalello, A.; Doglia, S. M.; Reymond, J. L. *J. Am. Chem. Soc.* **2008,** *130*, 17248-17249.

56. Abraham, M. J.; Murtola, T.; Schulz, R.; Páll, S.; Smith, J. C.; Hess, B.; Lindahl, E. *SoftwareX* **2015,** *1–2*, 19-25.

57. Roux, S.; Zekri, E.; Rousseau, B.; Paternostre, M.; Cintrat, J. C.; Fay, N. *J. Pept. Sci.* **2008,** *14*, 354-359.

Graphics for the Table of Contents: